

## DEVELOPMENT OF AN INTEGRATED CORE-EDGE SCENARIO USING THE SUPER H-MODE

T.M. WILKS, J.W. HUGHES, A. ROSENTHAL

Massachusetts Institute of Technology, Plasma Science and Fusion Center  
Cambridge, MA, USA  
Email: twilks@psfc.mit.edu

P.B. SNYDER, M. KNOLKER, D. ELTON, L. CASALI, T. OSBORNE, C. PAZ-SOLDAN, H. WANG

General Atomics  
San Diego, CA, USA

A. BORTOLON, F. EFFENBERG, B. GRIERSON, F.M. LAGGNER

Princeton Plasma Physics Laboratory  
Princeton, NJ, USA

C. LASNIER, A. MCLEAN, F. SCOTTI

Lawrence Livermore National Laboratory  
Livermore, CA, USA

J. WATKINS

Sandia National Laboratory  
Livermore, CA, USA

S. SAARELMA

Culham Centre for Fusion Energy  
Abingdon, UK

### Abstract

An optimized pedestal regime called the Super-H Mode (SH-mode) is leveraged to couple a fusion relevant core plasma with a high density scrape-off layer appropriate for realistic reactor exhaust solutions. Recent DIII-D experiments have expanded the operating space of the SH regime using advanced control algorithms and investigated optimization of impurity seeding, deuterium gas puffing, 3D magnetic perturbations, and plasma shape. Simultaneous regulation of the pedestal density and radiated power with in-vessel coils and nitrogen seeding enable optimal coupled divertor and pedestal conditions. Nitrogen seeding is used to establish a radiative mantle, leading to divertor temperatures of less than 15eV while maintaining SH-mode having marginal impact on pedestal and core performance. Increased levels of N<sub>2</sub> seeding facilitate the approach to detachment onset and divertor temperatures <5eV, with no degradation in stored energy, but with a 25% reduction in the electron temperature pedestal. Significant levels of N<sub>2</sub> seeding lead to partial detachment, which is so far associated with the loss of access to near Super H pedestal conditions.

Access to the SH-mode has been achieved in JET-like shapes on DIII-D with moderate plasma triangularity (average triangularity of 0.4, compared to typical values ~0.6), providing a pathway for increased performance for the JET campaign as well as increased confidence in the EPED predictions for SH-mode access in ITER.

### 1. THE SUPER H-MODE AS A PLATFORM FOR CORE-EDGE INTEGRATION STUDIES

A key challenge for extrapolating plasma regimes to future devices is how a fusion relevant core plasma can be coupled to a divertor solution. Successful integration would include, at minimum, a divertor that can handle extreme heat loads and particle fluxes. Additional considerations include the necessary baffling geometry for neutral fuelling and transport that is compatible with a high-performance core plasma with detached conditions [1-3]. In present devices, all these goals usually cannot be simultaneously met in standard H-mode scenarios. It is an active area of research to develop new target plasmas that push the limits on absolute pressure, triple product, stored energy, and heat fluxes to study how divertor closure and radiative mantles affect overall performance [4] with an end goal of developing a robust core-edge integrated regime that can be projected to future devices.

The Super H-mode (SH-mode) is a pedestal regime identified within the theoretical framework of the EPED model [5]. In specific regions of parameter space, a bifurcation occurs and EPED predicts two solutions for the pedestal pressure at a given density. Experimentally, a dynamic density trajectory and shape control are employed to reach this higher pressure branch of the solution [6]. The two solutions are separated by the SH channel, which decouples peeling and ballooning physics in the pedestal, and the plasma pressure continues to increase as a

function of density at much higher densities than it would without access to the SH channel. This positive scaling of pressure with density is favorable for reactor regimes because this enables 1) higher core pressures, which increases fusion power and 2) high density at the separatrix, which enables detached divertors [7-8].

The peeling-limited pressure pedestal reaches  $\sim 20\text{-}30\text{ kPa}$  on DIII-D [9] and up to  $\sim 80\text{ kPa}$  on C-Mod [10]. The pedestal maintains low collisionality ( $0.5 < \nu_e^* < 1$ ) with a high separatrix density ( $\sim 4 \times 10^{19}\text{ m}^{-3}$ ) for present devices [9], which is an ingredient for achieving a low heat flux to the divertor plate without degradation of the pedestal pressure. The SH regime provides a platform for quantitatively assessing trade-offs between high performance core plasmas coupled with radiative divertors on present devices. The theoretical framework for SH-mode allows predictive modelling of plasma scenarios to determine if small changes in quantities like triangularity,  $q_{95}$ , or  $\beta_N$  can have a large impact on potential pedestal and core performance by opening the Super H-mode channel. For example, EPED simulations and DIII-D experiments show small changes in JET-similar shapes provide a path towards SH-mode operation, and therefore potential for increased core pressures and stored energies in the upcoming D-T campaign.

An integrated core edge scenario using the SH-mode is presently being developed. The regime optimizes  $\text{N}_2$  seeding and density trajectories through advanced feedback algorithms that simultaneously optimize the line average density and divertor radiative power [12-13]. The  $\text{N}_2$  seeding rate is used as an actuator to impact localized power radiated in the divertor and scrape off layer regions measured by real-time bolometer signals. The pedestal density is measured by a scaled  $\text{CO}_2$  interferometer signal and actively controlled by  $\text{D}_2$  puffing (fuelling) and 3D magnetic perturbations from the I-coils (pump out). Introducing 3D magnetic perturbations that pump out particles to actively control the line average density allows the SH-mode plasmas to enter an extended stationary phase with sustained pedestal pressure and controlled impurity content during the flat-top of the discharge. The pedestal density profile is illustrated in Fig. 1a, showing the top of the pedestal being maintained by the I-coils, while the bottom of the pedestal and scrape off layer are separately controlled to increase the density near the divertor volume with  $\text{D}_2$  fuelling.

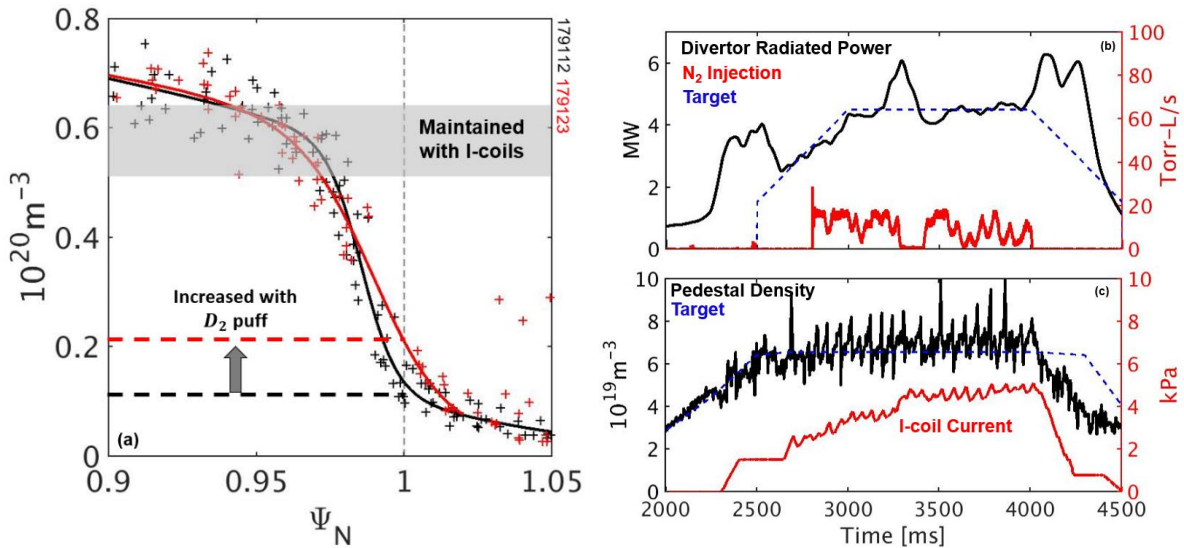


FIG 1: a) Pedestal electron density for two DIII-D Super H-mode discharges b) Time histories for radiated power, radiated power target, and nitrogen seeding rate c) pedestal density, pedestal density target, and I-coil current. Deuterium puffing acts to increase the electron density at the separatrix, and active feedback on the nitrogen seeding rate maintains a target radiated power in the divertor region. Feedback control on the I-coils pump-out particles to maintain the pedestal height.

The control schemes are illustrated in Fig 1bc. The radiated power (black) is shown in conjunction with the requested nitrogen gas flow (red) to meet the target (blue) in Fig. 1b. During a radiated power excursion, the gas flow request drops to zero to maintain the target value. Similarly, Fig. 1c shows the requested I-coils current (red) progressively increasing in order to maintain the target pedestal density. This discharge requires up to 5kA of I-coil current to maintain a pedestal density  $\sim 6.5 \times 10^{19}\text{ m}^{-3}$ . An optimal level of  $\text{N}_2$  and  $\text{D}_2$  are required to radiate power in the scrape off layer, but not collapse the pedestal. Realtime control has proven an effective and necessary tool to balance multiple core-edge integration objectives simultaneously.

## 2. COMPATIBILITY OF SUPER H-MODE WITH DETACHMENT

Experiments on DIII-D have employed co-current beam injection at magnetic fields in the range of  $B_t=2.1-2.2T$  and plasma currents in the range of  $I_p=1.4-2.0MA$  in both closed and open divertor configurations. Initial indications show that a slightly larger divertor volume with a longer leg between the x-point and strike points allows more power to be radiated in the scrape off layer and pedestal regions, and to be excluded from the core more effectively. Therefore, a series of discharges was made with varying power targets for radiated power for a lower biased double null ( $\delta_{avg} \sim 0.57$ ), with the strike point on the floor acting as a partially baffled divertor. Injection of deuterium and nitrogen lead to radiation in the scrape off layer and reduce the divertor heat flux and temperature to promote integration with requirements of plasma facing components. Table 1 summarizes three scenarios with different divertor conditions reflecting relative degrees of trade-off between core and divertor performance metrics low (4.5MW), medium (7.5MW), and high (8.5MW) levels for chosen for the radiated power target.

TABLE 1. CORE EDGE INTEGRATION TRADE OFFS IN SUPER H-MODE PLASMAS

Prad Target (shot)	$W_{MHD}$ (MJ)	$\beta_N$	$T_i^{ped}$ (eV)	$T_e^{ped}$ (eV)	ELMs	$T_e^{div}$ (eV)	$q_{div}$ (W/cm <sup>2</sup> )	Divertor Condition
0.0MW (184568)	2.1	2.5	1100	825	Regular Type I	60	480	Attached
4.5MW (177018)	1.7	2.1	750	900	Regular Type I	15	300	Attached
7.5MW (184569)	2.1	2.4	1000	620	Irregular Type I	< 5	350	Detachment Onset
8.5MW (184571)	1.5	1.8	900	450	Grassy	< 5	160	Partially detached (reduced momentum)

The pedestals associated with the plasma in Fig. 2a (4.5MW “low” seeding case) are well defined as Super H-mode in that the operating point is inside of the SH channel predicted by EPED, with  $\beta_N^{ped} \sim 1.0$ . However, there was not sufficient  $N_2$  injected to approach detachment, with a measured divertor temperature of  $\sim 15eV$  from the Divertor Thomson system [14]. The strike point requires temperatures  $< 5eV$  for processes such as ion-neutral elastic collisions and charge exchange to dominate ionization. Further experiments optimized the ratios of  $N_2$  and  $D_2$  to vary the density at the separatrix and radiation in the divertor, leading to the “medium” (184569) and “high” (184571) seeding cases summarized in Table 1.

At higher levels of  $N_2$  injection (184571), the divertor is cooled to  $< 5eV$  and the heat flux is mitigated during the detached phase; however, there is more penalty to the core and pedestal performance. This case is considered partially detached due to reduced momentum transport in the divertor and a “roll-over” in saturation current at the separatrix, yet there is still some plasma near the divertor plate. The 7.5MW radiated power target (184569) is a balance between divertor and core performance, where access to “near SH” and SH pedestals are maintained along with transient divertor detachment with temperatures  $< 5eV$ . This case is considered high recycling due to low divertor temperatures and at detachment onset because the divertor pressure is reduced compared to the reference scenario. “Near SH” access is defined by operation of the plasma on the peeling boundary in proximity of the SH channel entrance, but not robustly in the channel [15]. Fig. 2b shows heat flux profiles from IRTV [16] measurements corresponding to the discharges in Table 1 with increasing mitigation for the inner and outer strike points as more nitrogen is injected.

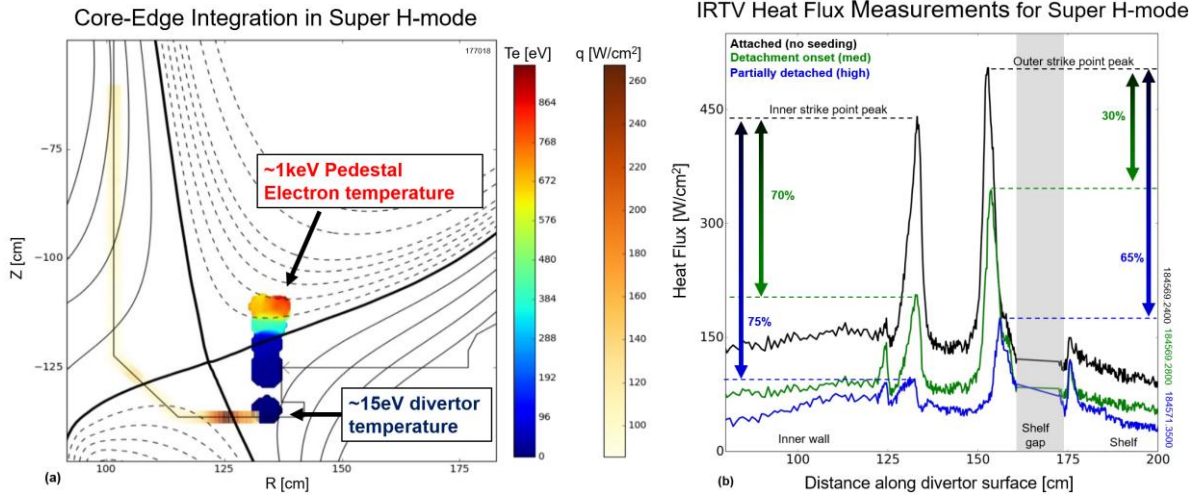


FIG 2: DIII-D divertor Thomson measurements in a Super H-mode with deuterium fuelling and nitrogen seeding. Pedestal electron temperatures are  $\sim 1\text{keV}$  and divertor temperatures are  $\sim 15\text{eV}$ . Infrared imaging heat flux measurements show reduced heat flux to the strike points due to a combination of  $\text{N}_2$  and  $\text{D}_2$  injection.

Two time histories are shown in Fig. 3 that have high stored energy ( $W_{MHD} > 2\text{MJ}$ ) and  $\beta_N (>2)$  in the core and are a) at detachment onset and b) partially detached, both behaving somewhat transiently. The “medium” seeded case has slightly better core and pedestal performance and the first few hundred milliseconds of the shaded region in Fig. 3a represents an optimal target for active feedback in future experiments. ELMs intermittently burn through the partially detached divertor, generating a dynamic pedestal with radiated power oscillating mostly below the total injected power, but sometimes exceeding it. The heat flux to the divertor is reduced by 30% compared to the no  $\text{N}_2$  reference.

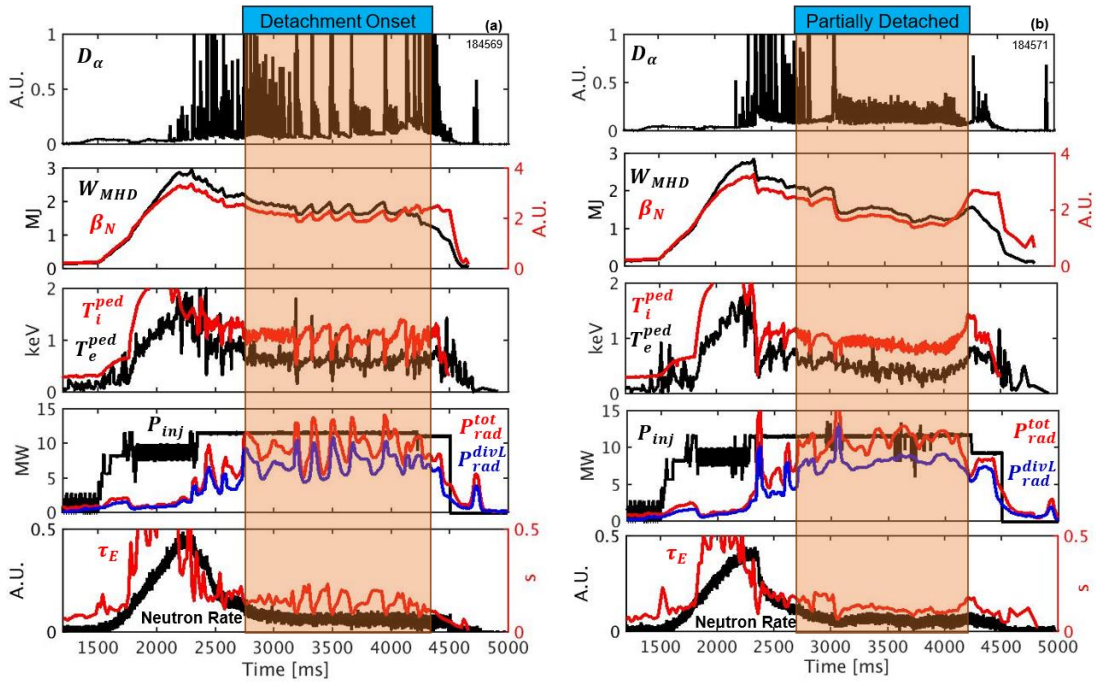


FIG 3: Time histories of near-SH plasmas that are a) at detachment onset and b) partially detached. Panels show divertor light, plasma stored energy and  $\beta_N$ , ion and electron pedestal temperatures, total injected power compared to radiated power, and stored energy and normalized neutron rate.

The “high” seeding case likely introduces excess  $\text{N}_2$ , but maintains quasi-stationary partial-detachment with small ELMs and stored energy of  $1.5\text{MJ}$  and  $\beta_N \sim 1.8$  for more than 1s. This operating point represents a slight trade off in core and pedestal performance for a robust divertor solution. The ELMs are small and do not

penetrate through the radiation front to the divertor, significantly reducing the heat flux (65%) as well as the temperature ( $<5\text{eV}$ ). Almost 100% of the injected power is radiated away as measured by bolometers before reaching plasma facing components. The electron temperature in the pedestal significantly degrades in this high seeding scenario to  $450\text{eV}$ , but the ion temperature pedestal is stationary at  $900\text{eV}$ .

The radiation measured from the Tangential TV system [17] for carbon and nitrogen emissions are shown in Fig. 4 for the “medium” seeded discharge (beginning of shaded region in Fig. 3a). The carbon radiation front, which can be associated with the main plasma, moves away from the strike point on the outboard side and close to the x-point and radiates  $\sim 10\text{eV}$ . The radiation from nitrogen is localized primarily to the strike point and cools the target plate to  $\sim 4\text{V}$ , indicating a transition to a high recycling regime.

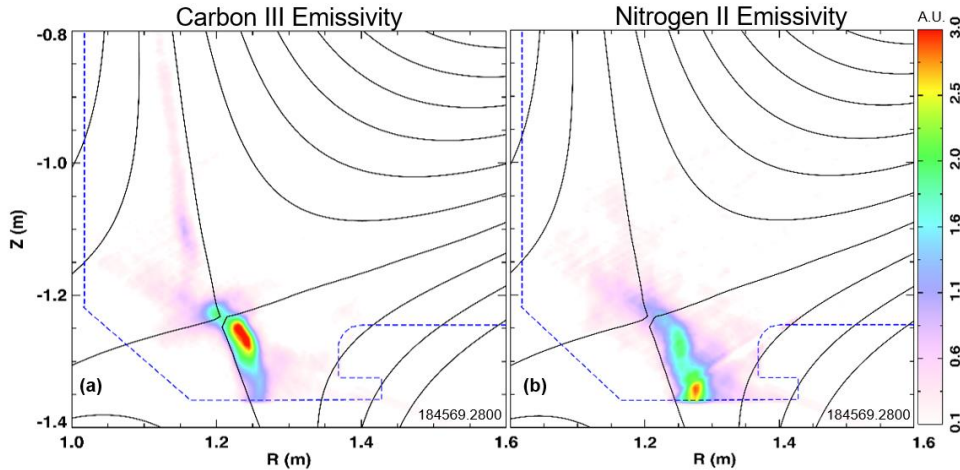


FIG 4: Tangential TV emissions for a) carbon and b) nitrogen radiation in a DIII-D near-SH-mode discharge. The carbon radiation front moves away from the strike point towards the x-point, and nitrogen is the dominant radiator at the strike point at detachment onset.

Langmuir probe [18] measurements show a progression into detached conditions for the SH core-edge integration scenarios in Fig. 5. The fully attached strike point (black) is greater than  $60\text{eV}$ , but when nitrogen is introduced, the temperature plummets to  $\sim 5\text{eV}$ , consistent with Tangential TV measurements. At detachment onset (green), the saturation current has a peak close to the separatrix, similar to the attached condition, but in the partially detached case (blue), this peak abates (or “rolls over” at the separatrix) and moves further into the scrape off layer. At detachment onset, the electron pressure decreases by  $\sim 30\%$ , indicating momentum loss from charge exchange.

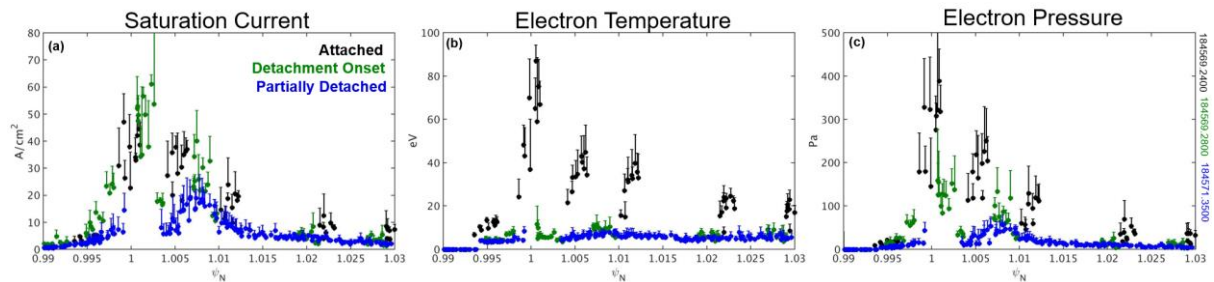


FIG 5: Inter-ELM Langmuir probe measurements showing attached (184569.2500), detachment onset (184569.2800), and partially detached (184571.3500) profiles for a) saturation current, b) electron temperature, and c) electron pressure in the scrape off layer and divertor region.

Progress is being made coupling a high performance core with divertor conditions approaching detachment requirements. Maximizing plasma current, magnetic field, plasma volume, and triangularity in conjunction with access to the Super H-mode provides a path towards maximized absolute plasma parameters such as pressure, stored energy, heat flux to the divertor on present devices, which is favorable for core edge integration studies. Future experiments can use different feedback target values or divertor geometries to further optimize the radiative divertor scenario. These variables will optimize localization of the nitrogen radiation away from the x-



point and constrain radiation to the scrape-off layer. A key optimization that is required for present devices is a large plasma volume to gain access to a high-performance core, but also a divertor volume large enough to radiate away the power outside the last closed flux surface, highlighting synergies with lines of research calling for more access to advanced divertor and long leg divertor configurations in future devices.

### 3. IMPACT OF PLASMA SHAPE ON SUPER H-MODE ACCESS AND PROJECTION TO JET

Plasma shape is a key parameter impacting pedestal stability, and when SH-mode access is marginal, small changes in triangularity and aspect ratio can lead to an increase in global metrics like plasma stored energy,  $W_{MHD}$ , through pedestal optimization. Previous experiments maximized plasma triangularity and volume in the SH regime in order to maximize pedestal and core performance; however, recent experiments show SH access can still be obtained at moderate plasma shaping [19]. Figure 6 shows the pedestal electron pressure and density in two JET similar shapes, with one having an increased plasma triangularity,  $\delta_{avg}$ , from 0.3 (gray) to 0.4 (red).

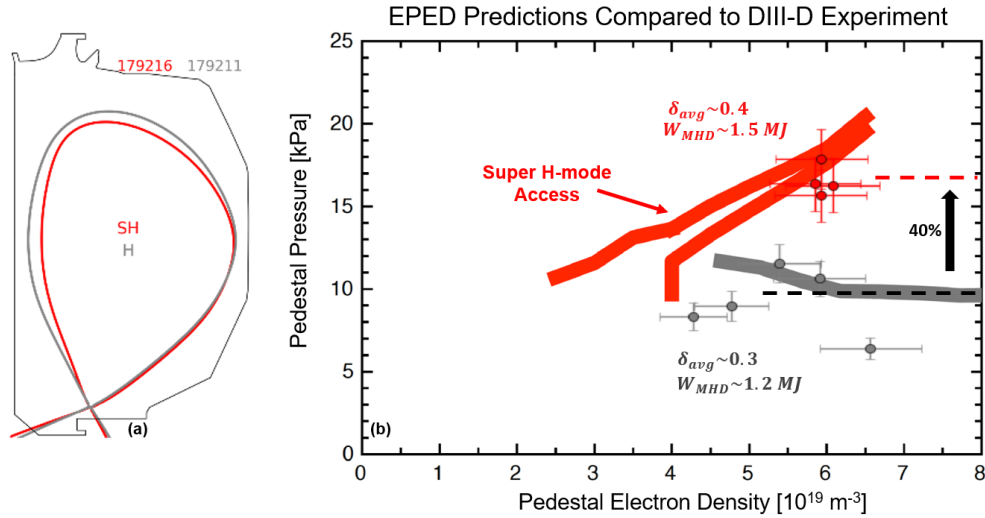


FIG 6: a) DIII-D plasma equilibria in JET-similar shapes with different triangularity, b) Density-pressure diagram showing Super H-mode channel access calculated from EPED compared to DIII-D experimental data in two JET similar shapes. The higher triangularity shape (red) exhibits SH-mode operation, but the lower plasma shaping case (gray) does not.

The change in triangularity opens access to the SH-mode channel, allowing a higher pedestal at the same density, and higher stored energy even with a slightly reduced plasma volume and lower plasma current. The red and gray EPED stability boundaries correspond to the different equilibria. The gray data points have a higher plasma current (1.5MA) compared to the red (1.3MA) as well as larger volume, which are generally more favorable for increased pedestal pressure, but SH access for the red equilibrium allows for a higher pedestal pressure. The  $\delta_{avg} \sim 0.3$  equilibrium is ballooning limited with a pedestal pressure  $\sim 10$  kPa, but with access to the SH channel on the peeling boundary, the equilibrium can reach pedestal pressures ( $p_{tot}^{ped} \sim 2p_e^{ped}$ ) consistently exceeding 15 kPa and approaching 20 kPa – almost a 100% increase at maximum. The relatively modest plasma triangularity compared to the double null SH experiments ( $\delta_{avg} \sim 0.6$ ) additionally leads to core pressures which are further from ideal  $\beta$  limits, allowing plasma trajectories deep in the SH channel to be maintained in a stationary state. Robust SH-mode access in lower single null shapes with intermediate levels of triangularity implies applicability for potential use as a target scenario in both JET and ITER. Figure 6 indicates that SH-mode is compatible with JET plasma shapes and that DIII-D experimental data aligns well with predictive EPED models for the JET scenario. The DIII-D plasmas in the JET shape exhibit a 25% increase of plasma stored energy and 40% increase in pedestal pressure, which indicates a potential for similar outcomes in JET plasmas at the same engineering parameters.

EPED predictions [10] for a high-performance JET scenario ( $I_p = 2.7 MA$ ,  $B_T = 2.8 T$ ) are shown in Fig. 7 with varied values of average triangularity of  $\delta_{avg} = [0., 0.25, 0.3, 0.45]$ . There is no SH channel access with  $\delta_{avg} \leq 0.3$ , but for  $\delta_{avg} = 0.45$ , a large channel is predicted. The SH channel is expected to open around pedestal densities of  $5 - 6 \times 10^{19} m^{-3}$ , with access to total pedestal pressures  $> 30$  kPa. Such a deep and broad SH channel represents potentially robust access to the SH regime for the JET. At the same engineering parameters,

but lower triangularity of  $\delta_{avg} \sim 0.3$ , the SH channel is seen to close, allowing maximum pedestal pressures only up to 18kPa.

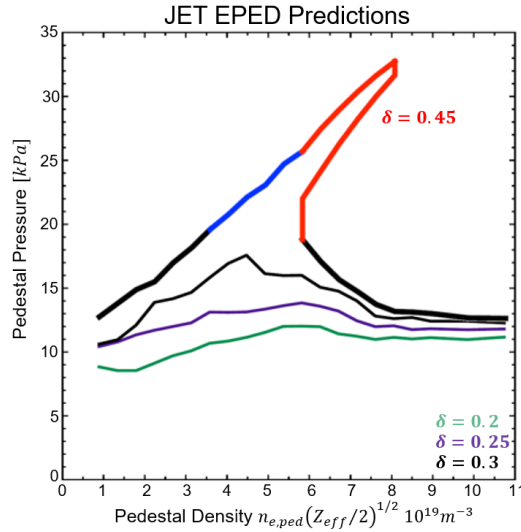


FIG 7: EPED prediction showing shape-dependent path to SH channel access for a JET high performance scenario with  $I_p = 2.7MA$  and  $B_T = 2.8T$  for average triangularities of 0.2, 0.25, and 0.45. With access to the SH channel, pedestals at a density  $\sim 6 \times 10^{19} m^{-3}$  have the potential to reach a 50% larger total pedestal pressure than the standard H-mode at the same density.

#### 4. CONCLUSIONS

Development of a plasma regime that successfully integrates a high-performance core with a robust divertor solution is essential for power producing devices. By simultaneously having low pedestal top collisionality and high separatrix density, the Super H-mode regime provides a platform to study the impacts of a high-performance core on divertor conditions in present devices. Advanced feedback algorithms for density and radiated power are enabling tools to achieve this goal experimentally. A validated theoretical framework provides confidence in projecting this regime to future devices, and the peeling physics the regime leverages in the pedestal is predicted to be ubiquitous in scaled reactor scenarios.

Using the Super H-mode, three different optimization avenues for core edge integration have been developed on DIII-D. Attached SH plasmas with high performance cores and pedestals ( $W_{MHD} \sim 2MJ$ ,  $\beta_N^{ped} > 1$ ), but modestly cooled divertors ( $T_e^{div} \sim 15eV$ ) represent a core-focused solution. A highly nitrogen seeded partially detached plasma with about 25% degradation to core performance ( $W_{MHD} \sim 1.5MJ$ ) represents a divertor-focused solution. A high recycling divertor at the onset of detachment with a modest penalties (<5%) to core performance, 30% reduced heat flux at the out outer strike point, and divertor temperatures  $\sim 5eV$  represents an interesting path towards a balanced solution.

DIII-D experiments coupled with EPED predictions demonstrate compatibility of the SH regime with low triangularity plasmas. Operation of the SH-mode at low triangularity has promising implications for compatibility with both ITER and JET. DIII-D experiments in a JET-similar shape show robust access to the SH channel, enabling an increase of stored energy by 25% with an increase of triangularity from 0.3 to 0.4. Dedicated EPED simulations for JET scenarios show a broad and deep channel accessible starting at  $5 - 6 \times 10^{19} m^{-3}$  for  $\delta = 0.45$ , but no access for the JET low triangularity scenario with  $\delta = 0.25$ . Increased performance for the JET D-T campaign could be enabled with thoughtful modifications to the scenario to enable access to the SH channel.

#### REFERENCES

- [1] LOARTE, A., Effects of divertor geometry on tokamak plasmas, Plasma Phys. Control. Fusion **43** (2001) R183.
- [2] CASALI, L., ELTON, D., BOEDO, J.A., LEONARD, T., AND COVELE, B., Neutral leakage, power dissipation and pedestal fueling in open vs closed divertors, Nucl. Fusion **60** 076011 (2020).
- [3] B. Lipschultz B. et al 1996 6th Int. Conf. on Fusion Energy p 425
- [4] CASALI, L., OSBORNE, T. H., GRIERSON, B. A., MCLEAN, A. G., MEIER, E. T., REN, J., SHAFER, M. W., WANG, H., AND WATKINS, J. G., Improved core-edge compatibility using impurity seeding in the small angle slot (SAS) divertor at DIII-D, Phys. Plasmas **27** 062506 (2020).

- [5] SNYDER, P.B., GROEBNER, R. J., LEONARD, A. W., OSBORNE, T. H., AND WILSON, H. R., Development and validation of a predictive model for the pedestal height, *Phys. Plasmas* **16** 056118 (2009).
- [6] SOLOMON, W.M., SNYDER, P. B., BURRELL, K. H., FENSTERMACHER, M. E., GAROFALO, A. M., GRIERSON, B. A., LOARTE, A., MCKEE, G. R., NAZIKIAN, R., AND OSBORNE, T. H., Access to a new plasma edge state with high density and pressures using the quiescent H-mode, *Phys. Rev. Lett.* **113** 135001 (2014).
- [7] CASALI, L., SANG, C., MOSER, A.L., COVELE, B.M., GUO, H.Y., SAMUEL, C., Modelling the effect of divertor closure on detachment onset in DIII-D with the SOLPS code, *Contrib. Plasma Phys.* **58** (2018) 725-731.
- [8] MOSER, A., CASALI, L., COVELE, B. M., LEONARD, A. W., MCLEAN, A. G., SHAFER, M. W., WANG, H. Q., AND WATKINS, J. G., Separating divertor closure effects on divertor detachment and pedestal shape in DIII-D, *Phys. Plasmas* **27** 032506 (2020).
- [9] SNYDER, P.B., HUGHES, J.W., OSBORNE, T.H., PAZ-SOLDAN, C., SOLOMON, W.M., KNOLKER, M., ELDON, D., EVANS, T., GOLFINOPOULOS, T., GRIERSON, B.A., GROEBNER, R.J., HUBBARD, A.E., KOLEMEN, E., LABOMBARD, B., LAGGNER, F.M., MENEGHINI, O., MORDIJK, S., PETRIE, T., SCOTT, S., WANG, H.Q., WILSON, H.R., AND ZHU, Y.B., High fusion performance in Super H-mode experiments on Alcator C-Mod and DIII-D, *Nucl. Fusion* **59** 086017 (2019).
- [10] HUGHES, J., SNYDER, P.B., REINKE, M.L., LABOMBARD, B., MORDIJK, S., SCOTT, S., TOLMAN, E., BAEK, S.G., GOLFINOPOULOS, T., GRANETZ, R.S., GREENWALD, M., HUBBARD, A.E., MARMAR, E., RICE, J.E., WHITE, A.E., WHYTE, D.G., WILKS, T., AND WOLFE, S., Access to pedestal pressure relevant to burning plasmas on the high magnetic field tokamak Alcator C-Mod, *Nucl. Fusion* **58** 112003 (2018).
- [11] KALLENBACH, A., BERNERT, M., DUX, R., CASALI, L., EICH, T., GIANNONE, L., HERRMANN, A., MCDERMOTT, R., MLYNEK, A., MÜLLER, H. W., REIMOLD, F., SCHWEINZER, J., SERTOLI, M., TARDINI, G., TREUTTERER, W., VIEZZER, E., WENNINGER, R., WISCHMEIER, M., Impurity seeding for tokamak power exhaust: from present devices via ITER to DEMO, *Plasma Phys. Control. Fusion* **55** 124041 (2013).
- [12] ELDON, D., KOLEMEN, D.A., HUMPHREYS, HYATT, A. W., JÄRVINEN, A.E., LEONARD, A.W., MCLEAN, A.G., MOSER, A.L., PETRIE, T.W., WALKER, M.L., Advances in radiated power control at DIII-D, *Nucl. Mater. and Energy* **18** (2019) 285-290.
- [13] LAGGNER, F., ELDON, D., NELSON, A.O., PAZ-SOLDAN, C., BORTOLON, A., EVANS, T.E., FENSTERMACHER, M.E., GRIERSON, B.A., HU, Q., HUMPHREYS, D.A., HYATT, A.W., NAZIKIAN, R., MENEGHINI, O., SNYDER, P.B., UNTERBERG, E.A., KOLEMEN, E., Real-time pedestal optimization and ELM control with 3D fields and gas flows on DIII-D, *Nucl. Fusion* **60** 076004 (2020).
- [14] GLASS, F., CARLSTROM, T. N., DU, D., MCLEAN, A. G., TAUSSIG, D. A., AND BOIVIN, R. L., Upgraded divertor Thomson scattering system on DIII-D, *Rev. Sci. Instrum.* **87** 11E508 (2016).
- [15] KNOLKER, M., EVANS, T. E., SNYDER, P. B., GRIERSON, B., HANSON, J., JAERVINEN, A., JIAN, X., MCCLENAGHAN, J., OSBORNE, T., PAZ-SOLDAN, C., SOLOMON, W., AND WILKS, T., On the stability and stationarity of the Super H-mode combined with an ion transport barrier in the core, *Plasma Phys. Control. Fusion* **63** 025017 (2021).
- [16] LASNIER, C.J., ALLEN, S. L., ELLIS, R. E., FENSTERMACHER, M. E., MCLEAN, A. G., MEYER, W. H., MORRIS, K., SEPPALA, L. G., CRABTREE, K., AND VAN ZEELAND, M. A., Wide-angle ITER-prototype tangential infrared and visible viewing system for DIII-D, *Rev. Sci. Instrum.* **85** 11D855 (2014).
- [17] FENSTERMACHER, M.E., MEYER, W. H., WOOD, R. D., NILSON, D. G., AND ELLIS, R., A tangentially viewing visible TV system for the DIII-D divertor, *Rev. Sci. Instrum.* **68** 974 (1997).
- [18] WATKINS, J. G., TAUSSIG, D., BOIVIN, R. L., MAHDAVI, M. A., AND NYGREN, R. E., High heat flux Langmuir probe array for the DIII-D divertor plates, *Rev. Sci. Instrum.* **79** 10F125 (2008).
- [19] KNOLKER, M., SNYDER, P. B., EVANS, T. E., WILKS, T., ELDON, D., GRIERSON, B., JAERVINEN, A., JIAN, X., LAGGNER, F., MCCLENAGHAN, J., MCLEAN, A. G., OSBORNE, T., PAZ-SOLDAN, C., SCOTTI, F., AND SOLOMON, W., Optimizing the Super H-mode pedestal to improve performance and facilitate divertor integration, *Phys. Plasmas* **27** 102506 (2020).

#### ACKNOWLEDGEMENTS

The efforts of the DIII-D team were essential to this work and greatly appreciated. This research was supported by the U.S. Department of Energy, Office of Science, and Office of Fusion Energy Sciences using the DIII-D National Fusion Facility under awards DE-FC02-04ER54698 and MIT cooperative agreement DE-SC0014264. Additional work supported by the U.S. Department of Energy under DE-FG02-95ER54309, DE-AC52-07NA27344, DE-AC02-09CH11466, DE-AC02-05CH11231, and DE-NA0003525.

#### DISCLAIMER

This report was prepared as an account of work sponsored by an agency of the United States Government. Neither the United States Government nor any agency thereof, nor any of their employees, makes any warranty, express or implied, or assumes any legal liability or responsibility for the accuracy, completeness, or usefulness of any information, apparatus, product, or process disclosed, or represents that its use would not infringe privately owned rights. Reference herein to any specific commercial product, process, or service by trade name, trademark, manufacturer, or otherwise, does not necessarily constitute or imply its endorsement, recommendation, or favoring by the United States Government or any agency thereof. The views and opinions of authors expressed herein do not necessarily state or reflect those of the United States Government or any agency thereof.